Journal of ASTM International, Vol. 9, No. 5
Paper ID JAI104091
Available online at www.astm.org

Christopher C. White,[1] *Donald L. Hunston,*[2] *Kar Tean Tan,*[2] *James J. Filliben,*[3] *Adam L. Pintar,*[3] *and Greg Schueneman*[4]

A Systematic Approach to the Study of Accelerated Weathering of Building Joint Sealants*

ABSTRACT: An accurate service life prediction model is needed for building joint sealants in order to greatly reduce the time to market of a new product and reduce the risk of introducing a poorly performing product into the marketplace. A stepping stone to the success of this effort is the precise control of environmental variables in a laboratory accelerated test apparatus in order to produce reliable weathering data that can be used to generate a predictive model. This contribution reports a systematic study, using a novel laboratory test apparatus, investigating the individual and synergistic impacts of four environmental factors (cyclic movement, temperature, relative humidity, and ultraviolet radiation) on the durability of a sealant system. The apparatus used is unique because it not only allows the precise control of environmental factors but also permits in situ characterization tests so that the specimens need not be removed from the apparatus chamber. Graphical and quantitative statistical approaches have been used to analyze the data. The study shows that the critical role of each individual factor, as well as synergism among the different factors, can be readily quantified, and modes of degradation possibly can be identified.

KEYWORDS: Sealant, Service Life Prediction, model, construction, modulus, SPHERE, Statistics

Introduction

The accurate prediction of in-service performance in less time than is required for field tests and tests on structures has remained a modern unresolved scientific issue. Reliable performance data still require long-term field exposure. Such tests are needed in order to decrease the risk of introducing a poorly performing product into the marketplace. However, the cost of developing new products is directly related to the product development time and the time to market. The more time a product spends in the pipeline, the greater investment required and the smaller the eventual profit. Furthermore, long test times clearly hamper product innovations. Therefore, extensive efforts have been made to design short-term tests that provide an accurate indication of how well a sealant will perform in actual use. Although modern commercial sealants typically are designed to last for 20 years or more, studies in the construction industry have found a 50 % failure rate in less than 10 years and a 95 % failure rate within 20 years after installation [1–3]. These findings clearly show the inadequacy of current accelerated test methods and the need for the development of a reliable service life prediction methodology based on improved accelerated test methods.

The difficulties that hinder efforts to relate field and laboratory results include (a) unresolved differences between, and a poor understanding of, the failure modes in the two environments [4–6] and (b) a lack of methods with which to accurately quantify the effects of the environmental degradation factors in laboratory and field tests [4,5]. In particular, visual evaluation of physical performance, including crack and chip size, chalking behavior, and color change, is one of the main tests for the effects of weathering [7–9]. Although

Manuscript received June 7, 2011; accepted for publication February 29, 2012; published online May 2012.
[1]National Institute of Standards and Technology, Engineering Laboratory, Materials and Structural Systems Division, 100 Bureau Dr., Stop 8615, Gaithersburg, MD 20899-8615 (Corresponding author), e-mail: christopher.white@nist.gov
[2]National Institute of Standards and Technology, Engineering Laboratory, Materials and Structural Systems Division, 100 Bureau Dr., Stop 8615, Gaithersburg, MD 20899-8615.
[3]National Institute of Standards and Technology, Information Technology Laboratory, Statistical Engineering Division, 100 Bureau Dr., Stop 0001, Gaithersburg, MD 20899-0001.
[4]Forest Products Laboratory, 1 Gifford Pinchot Dr., Madison, WI 53726.
*Certain commercial products or equipment are described in this paper in order to specify adequately the experimental procedure. In no case does such identification imply a recommendation or endorsement by the National Institute of Standards and Technology (NIST), nor does it imply that the mentioned item is necessarily the best available for the purpose.

such a methodology might relate to a customer-perceived failure mode, it is qualitative and time consuming and provides little insight into the mechanisms leading to these macroscopic changes. In this paper and in previous reports [10–19], many of these issues have been resolved. Previous studies examined the impact of temperature [10–17], humidity [13,16–18], applied static and dynamic strain [18], and outdoor field exposure [10,14,15,17,19] on the durability of sealants, and they also reported the design of novel laboratory and field testing devices [14,15,19,20]. The success of this endeavor depends upon the use of a reliability-based methodology to make rapid, precise, and accurate environmental performance predictions. In this paper, we consider only the problem of identifying and ranking important degradation factors.

The research reported here represents a continuing effort in predicting the service life of building joint sealants. Although temperature, relative humidity, ultraviolet (UV) radiation, and cyclic movement have been identified as prevalent aging factors for sealants [21], there is no study thus far that systematically and quantitatively shows the impact of these environmental factors when they are acting either independently or synergistically on sealant properties. The objective of this study, therefore, is to design a systematic accelerated protocol that can provide a quantitative platform for investigating the individual and synergistic impacts of environmental factors. The study employs a custom-made laboratory apparatus with the capability to control these four environmental factors to high levels of accuracy, precision, and reproducibility [20]. Moreover, because the deformation can be controlled, in situ mechanical characterization tests can be performed without removing specimens from the chamber. Thus, this method permits comparison of the dose of laboratory degrading factors in a quantitative manner. It is demonstrated that the individual and synergistic effects of factors on the durability of sealants can be revealed using this reliability-based approach. The wealth of data generated from the study is expected to facilitate the prediction of potential failure modes and the generation of a service life prediction model for sealant materials.

Experiment

Materials and Specimen Preparation

A commercial sealant, provided by a member of a National Institute of Standards and Technology/industry consortium,[5] was fabricated into sealant joints conforming to ASTM C719 [22] (Fig. 1). The chemistry of the sealant tested was unknown, but physical examination and testing revealed an elastomeric behavior typical of sealants, and the specimen had a white, opaque appearance.

Exposure Conditions and Characterization

The four custom-built sealant testing chambers employed in this study have the ability to independently control temperature (±0.2°C), relative humidity (RH) (±0.5 %), UV radiation, and cyclic movement. Because the deformation can be controlled, mechanical characterization tests can be performed without removing the specimens from the chamber. A full description of the chamber design is documented elsewhere [20]. The temperature was controlled with a precision temperature regulator, humidity control was accomplished via proportional mixing of dry and saturated air, and a highly uniform flux of UV radiation was attained by attaching the chambers to an integrating sphere-based radiation source (simulated photodegradation via high energy radiant exposure [SPHERE] [23]). The SPHERE is equipped with a microwave-powered lamp system consisting of six VPS/I600-60 lamp modules. Partially enclosing each light source is a dichroic mirror that removes almost all of the thermal radiant energy (i.e., visible and infrared radiation) from the beam while reflecting the spectra UV emissions into the SPHERE. Thus, without external heating, the temperature in the chamber is about 27°C ± 2°C. A cut-off filter is positioned between the light source assemblage and the SPHERE that prevents almost all of the radiation below

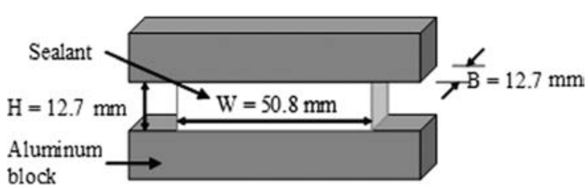

FIG. 1—*Schematic illustration of the test specimen geometry used (not to scale).*

290 nm from entering the SPHERE. It should be noted that no attempt was made in this study to simulate the full spectrum of terrestrial solar radiation or the spectra power distribution of the UV portion of such. Thus, the sealants were exposed to an output in the spectral region between 290 nm and 450 nm and an irradiance of approximately 500 W/m^2. A comparison of the spectral power distribution of the SPHERE radiation source with the reference solar UV spectral distribution from ASTM G173-03 [24] is shown in Fig. 2. Hereinafter, the radiation is referred to as UV for simplicity.

The sealant specimen was attached between a fixed and a movable grip with a computer-controlled stepper motor and a transmission system providing precise movement control. Each chamber had two motors, with four specimen holders on each motor, for a total of eight specimen holders. Each specimen holder was attached to a hermetically sealed load cell with a capacity of ±113.4 kg. Two linear variable differential transformers (LVDTs), one for each motor, with a deflection range of ±6.35 mm were used to measure sealant movement. Data from load cells and LVDTs were fed directly into a Keithley 2701 ethernet-based data acquisition system. A custom LabVIEW program was written to collect the voltage measurements from the Keithley system every 15 s. The data were averaged once per minute and appended to a tab-delimited database on a remote server.

Data

There were four exposure variables: temperature, RH, cyclic movement, and UV radiation. In all cases, the exposure time was fixed at 1 month. The air temperature was held at 30°C, 40°C, or 50°C. The RH was maintained at 0 %, 25 %, 50 %, or 75 %. Note that exposure to higher levels of RH, liquid water (which allows the possibility for the abstraction of components in the sealants), and freezing conditions is an important area that is not covered in the current study. The deformation involved cyclic movement in a triangular wave varying from 0 % strain to a prescribed maximum strain level at a rate of 38 min/cycle. The maximum strain level was 0 %, 8 %, 15 %, or 25 %. The UV radiation was either on or off. Of 96 possible conditions in the full factorial experimental design, 54 were investigated. These conditions generated a total of 312 data points, which were subsequently trimmed down to 293 after data cleaning to remove out-of-range or suspicious values resulting from faulty collection.

Prior to and after the exposure tests, the specimens were allowed to recover and the mechanical properties of each were characterized at room temperature. The specimens first were subjected to two loading-unloading-recovery cycles at a maximum strain of 26 %. This was followed by a stress relaxation measurement at a strain of 18 %. The strain history used is shown schematically in Fig. 3. The loading-unloading tests utilized a crosshead speed of 2.64 mm/min, so the total time under load was 150 s. To allow for viscoelastic recovery, the specimen was held at 0 % strain for 1500 s before the next step.

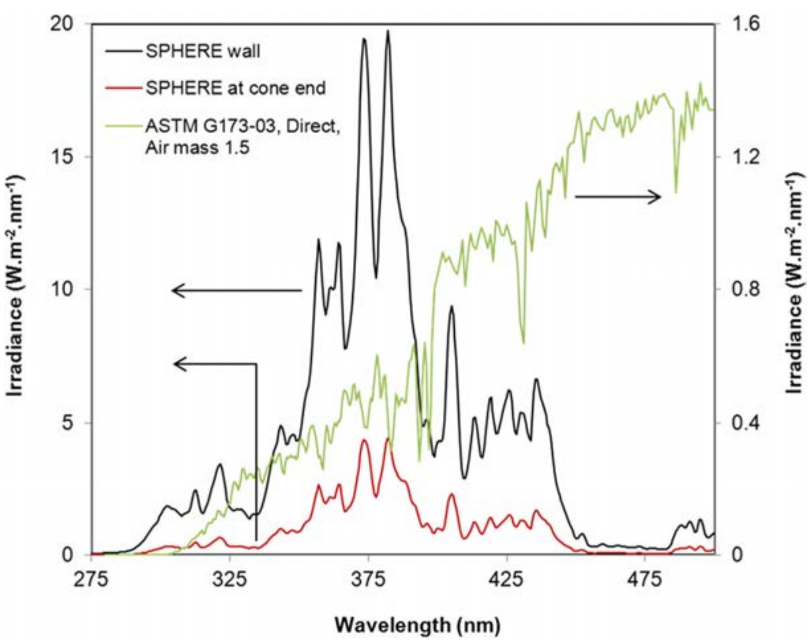

FIG. 2—*Comparison of the irradiance of SPHERE and the ASTM G173-03 solar spectrum.*

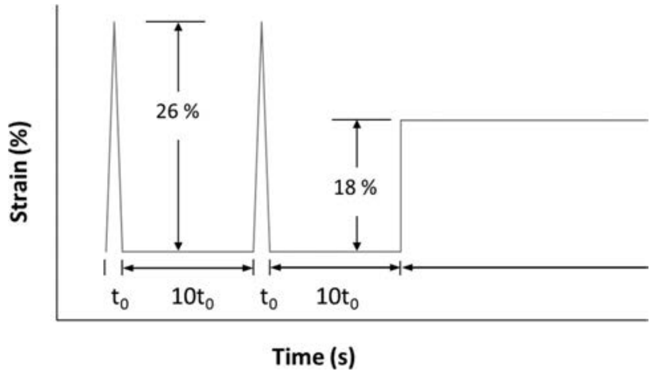

FIG. 3—*Strain history used for Mullins cycles and stress relaxation tests.*

The purpose of the two loading-unloading cycles was to quantify the Mullins effect and eliminate its influence in the subsequent characterization test. In stress relaxation measurements, the crosshead speed was 70 mm/min, which meant that the specimen reached the hold strain in just under 2 s. In order to allow for non-instantaneous loading, data points during the first 15 s were ignored.

From the stress relaxation data, an apparent modulus E_a was calculated using a relationship based on the statistical theory of rubberlike elasticity [25–27].

$$E_a(t,\lambda) = \frac{3L(t)}{WB(\lambda - \lambda^{-2})} \tag{1}$$

where:

W and B = width and breadth of the sealant (Fig. 1), respectively,
L = load,
t = time, and
λ = extension ratio, which is given by

$$\lambda = 1 + \frac{\Delta}{H} \tag{2}$$

where:

Δ = crosshead displacement, and
H = undeformed height of the sealant.

From this information, an apparent modulus versus time curve is generated. The magnitude and time dependence of this apparent modulus are related to the molecular structure of the sealant. If the changes in this modulus with exposure time are monitored in a degradation experiment, changes in the molecular structure of the sealant can be estimated. Changes in the modulus over time also provide crucial information about how a sealant responds to the stresses imposed by the expansion and contraction of a structure over the diurnal cycle. A modulus ratio F was used to characterize the effect of the environment on E_a.

$$F = \frac{E_a(t)}{E_{a,0}(t)} \tag{3}$$

in which $E_a(t)$ and $E_{a,0}(t)$ are the apparent moduli before and after exposures, respectively.

The relative effects of the various environmental factors can also depend on the type of evaluation used as the criterion of failure. We believe that changes in the modulus are a clear indication that there are chemical and mechanical changes occurring in the sealant. Initially, these changes might be either detrimental or beneficial to sealant performance, but eventually, if the changes become large enough, the performance will likely deteriorate. For the particular material tested here, we have found that a decrease in the modulus is a precursor to cracking and debonding, which would allow moisture penetration (the usual definition of failure).

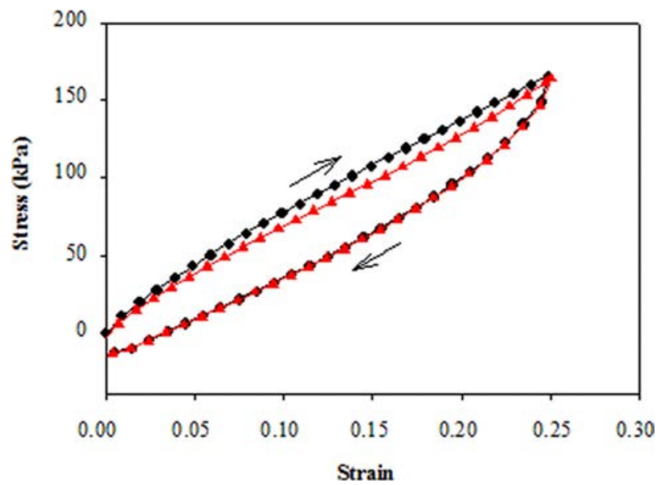

FIG. 4—*Loading-unloading tests on a fresh specimen at a crosshead speed of 2.64 mm/min to a max strain of 25 %. Circles and triangles represent the first and second loading cycles, respectively. Arrows indicate the loading-unloading directions.*

Results and Discussion

Mullins Effect

As mentioned, the characterization tests involved two load-unload-recovery cycles so as to examine the Mullins effect. Typical results for the stress-strain curves generated with a fresh sample are shown in Fig. 4. Like other rubberlike materials, these sealants exhibit a strong Mullins effect in that there is a significant reduction in the stress at a given strain level during the second loading, as compared to the stress level on the first loading. The unloading curves, however, are identical.

Stress Relaxation Behavior

Apparent moduli versus relaxation time curves for specimens before and after exposure to motion at 25 % maximum strain, 75 % RH, and 30°C and with UV radiation are shown in Fig. 5(*a*). The curves represent the average of up to four replicates, and the vertical bars indicate one standard deviation. The difference seen in Fig. 5(*a*) between the two curves is significant. Note that there is no change in the curve shape,

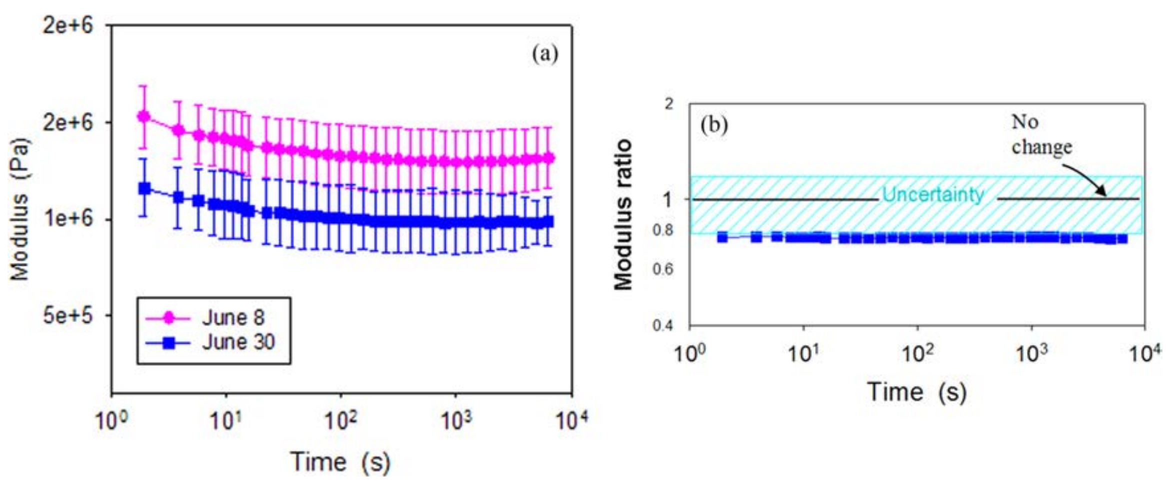

FIG. 5—*(a) Variation of apparent modulus as a function of relaxation time for the sealant under conditions of 25 % max strain/30°C/75 % RH before and after exposures. The error bars represent one standard deviation from mean values. (b) Variation of modulus ratio as a function of relaxation time for the sealant under the same conditions as in (a) before and after exposures. The hashed region represents the combined experimental error from the data before and after exposures. If the points for a given curve fall within this region, there is no change in the experimental uncertainty.*

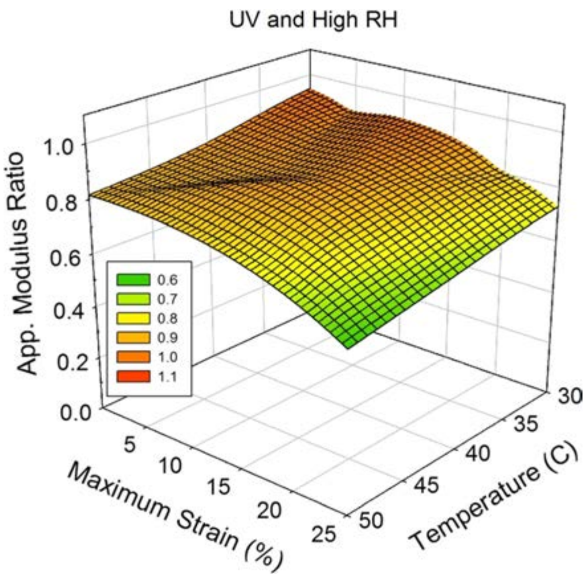

FIG. 6—*Dependence of modulus ratio on max strain and temperature for specimens exposed to UV radiation and high RH (75 %).*

implying that the time dependence of the apparent modulus is very similar before and after exposures. However, the magnitude of the apparent modulus decreased by a small amount after exposure. In order to facilitate comparison between different exposure conditions, stress relaxation data are presented as a modulus ratio (F) as a function of the relaxation time [Eq 3, Fig. 5(*b*)]. In such a graph, no change would be represented by a horizontal straight line at $F = 1$. A horizontal line above or below $F = 1$ indicates that exposure caused a vertical shift in the stress relaxation curve but no change in shape; i.e., the time dependence did not change. Something other than a horizontal straight line indicates a change in the time dependence. The experimental uncertainty can be shown as a hashed region on either side of $F = 1$, so if the points for a given curve fall within this region, there are no changes outside the experimental uncertainty.

Data Analysis

One approach to examining the results is the use of 3D graphs such as that shown in Fig. 6, which plots the apparent modulus ratio against the temperature and the maximum strain in the cyclic movement during 1 month of exposure at 75 % RH with UV radiation. The graph shows that both motion and temperature produce a significant reduction in the modulus for the range of conditions tested. Moreover, the effects are synergistic in that the combination of motion and temperature produced a larger reduction in modulus than that seen for either variable alone.

This approach is useful for illustrating general trends and highlighting the nature of the response surface. However, as the goal of this paper is to identify and rank environmental factors that are important to sealant degradation, we take a different approach to the data analysis. More specifically, design of experiments (dex) scatter plots, dex mean plots, analysis of variance (ANOVA), and block plots [28] are used. Of all of these statistical techniques, the block plot bears the most weight.

dex Plots

Figure 7(*a*) shows the dex scatter plot of the data. The vertical axis is the modulus ratio in, and the horizontal axis depicts the four exposure variables, i.e., three-level temperature, four-level cyclic movement, four-level RH, and two-level UV exposure. It can be seen that there is no apparent relationship between the modulus ratio and the four exposure variables due to large differences in the modulus ratio for a given setting of exposure variable.

In contrast, the dex mean plot [Fig. 7(*b*)], which shows the mean values of the modulus ratio for various levels of each exposure variable, reveals that all exposure variables have an effect on modulus decrease. A relation between the change in modulus ratio and exposure to the various environmental variables is evident, suggesting that the presence of UV radiation, an increase in temperature, a larger cyclic movement, or increased RH leads to a decrease in the modulus ratio for the particular sealant tested here.

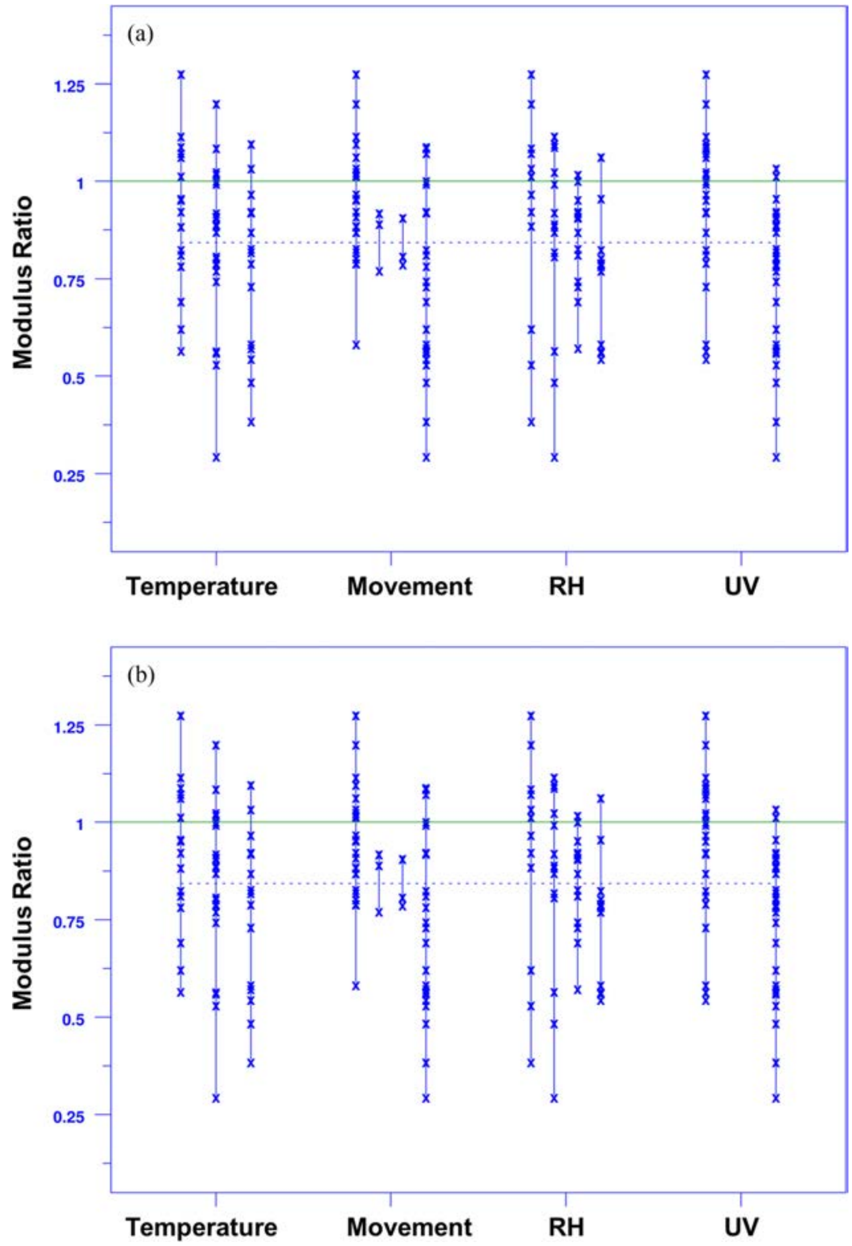

FIG. 7—*(a) dex scatter plot and (b) mean plot of data for various exposure conditions. Although no obvious relationship between the modulus ratio and exposure variables is present in the dex scatter plot, the mean plot reveals that all exposure variables seem important for modulus decrease.*

The effects of all of the exposure variables on the modulus decrease are evident, with cyclic movement and UV being the most important factors.

ANOVA

ANOVA, with main effects only, was used to compare the effects of temperature, cyclic movement, RH, and UV on the modulus ratio. Statistical significance was set at the conventional 5 % level. Table 1 summarizes the results of ANOVA. *F*-tests show a significant effect of UV, cyclic movement, and RH on the modulus decrease; however, ANOVA fails to reveal a significant impact of temperature on the modulus decrease at the 5 % level. We find this result unbelievable after looking at the dex plots, and it might be due to at least one of the following assumptions' being faulty: normality, homogeneity of variance, independence, or no interactions.

With the above ANOVA caveats in mind, we may form, based on the significance levels, the following ranked list of factors: (1) cyclic movement, (2) UV, (3) RH, and (4) temperature. Because of the

TABLE 1—ANOVA results.

Exposure Variable	Degrees of Freedom	Sum of Squares	Mean Squares	*F* Value	Pr (F)
Temperature	4	0.69060	0.172651	1.466906	0.2131036
Relative humidity	3	1.31257	0.4375124	3.717369	0.0122131
Cyclic movement	3	1.92587	0.641956	5.454293	0.0012248
UV	1	1.10464	1.104640	9.385429	0.0024503
Residuals	228	26.83499	0.117697		

caveats, we use the second statistical method (block plots) to assess factor significance and form a ranked list of importance.

Block Plots

A sensitivity analysis based on block plots was performed [28–30]. Block plots assess whether the factor of interest (known as the target factor) has a statistically significant effect on the decreasing mean modulus ratio, and whether that conclusion about the target factor is valid robustly or unconditionally over all other non-target factors (known as robustness factors) in the experiment. The block plot is essentially a character plot with the boxes superimposed for each setting in order to force attention on the within-box target values, as opposed to the between-box differences. It is an excellent graphics tool for robustly assessing the importance of each individual factor.

Effect of Temperature

Figure 8(*a*) displays the block plot targeting temperature (i.e., 30°C, 40°C, and 50°C) over 22 distinct combinations of RH, cyclic movement, and UV radiation. In this plot, temperature is the target factor (as denoted by the plot character), and UV radiation, cyclic movement, and RH are all robustness factors. The vertical axis shows the magnitude of modulus ratio, and the horizontal axis comprises various combinations of the three robustness factors. In order to facilitate comparison among different exposure conditions, the mean modulus ratio is determined by averaging the modulus ratio at the same temperature within each bar and is displayed in Fig. 8(*b*). For example, the first bar shows the effect of temperature on the modulus for the 0 % RH/no cyclic movement/no UV condition. Note that a temperature of 30°C yields a modulus ratio of ≈1.25 and thus an increase of 25 %, whereas 50°C yields a 13 % decrease. For the second bar (i.e., the combination of 0 % RH and UV radiation without cyclic movement), the sealants exhibit modulus increases, but the magnitude of increase is comparatively less than those in the first bar. However, a lower decrease in the modulus of 25 % is observed for exposures at 50°C.

Scanning across the various robustness factor settings (horizontally), it can be seen that 40°C or 50°C is almost always located at the bottom of each bar, and that the corresponding modulus ratios are almost always below unity. Indeed, 14 of the 16 robustness factor settings show that elevated temperature exposures of either 40°C or 50°C result in a greater modulus reduction than those at 30°C. In order to quantify whether temperature is statistically significant over all robustness factor settings, the chance for 14 of the 16 robustness factor settings showing the importance of the temperature effect involving randomness is calculated using a binomial model.

$$P(x,n,p) = \binom{n}{x} p^x (1-p)^{n-x} \tag{4}$$

where:

x = number of successes in n trials, and

p = probability of success in a single trial.

The probability of obtaining at least 14 of the 16 robustness factor settings under the null hypothesis of $p = 0.5$ is ∼0.2 %. Such a low probability event is rejected as unrealistic, allowing the conclusion that elevated temperature is statistically significant in decreasing modulus irrespective of the robustness factor settings. The importance of the temperature effect is supported further by Fig. 9(*a*), which shows the values of the modulus ratio for different temperatures arranged in order of increasing magnitude for

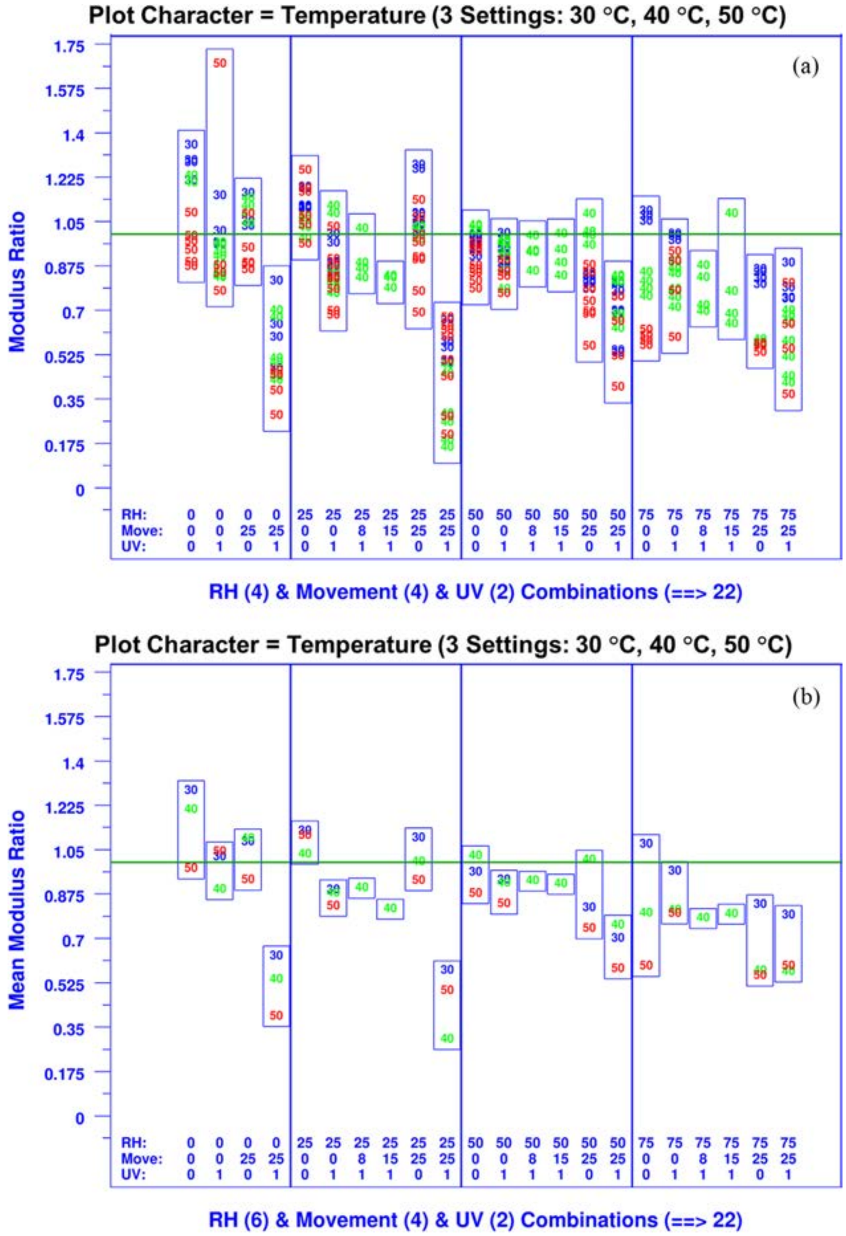

FIG. 8—*Block plot of (a) modulus ratio and (b) mean modulus ratio targeting temperature across 22 distinct combinations of RH, cyclic movement, and UV. Consistencies in terms of the local arrangement of 40°C or 50°C movement within each bar and large block heights over all settings of robustness factors show the deleterious effect of elevated temperatures on modulus reduction.*

54 combinations of exposure conditions. It is evident that modulus data for 40°C or 50°C are always located at the bottom left corner of the plot, which indicates a lower modulus. Moreover, there is a large "local" (i.e., for that particular combination of robustness factors) temperature effect on modulus reduction, which is manifested in the large within-block difference (i.e., tall blocks). The existence of (a) consistently large block heights and (b) consistent temperature arrangement within blocks demonstrates that the temperature effect on modulus reduction is important. Note that less important factors will have only one of these two properties, and unimportant factors will have neither.

The decrease in sealant modulus as a function of exposure temperature suggests that chain scission is more likely than cross-linking as the dominant degradation mode. Thermally enhanced chain scission may be attributed to an increase in the average kinetic energy of polymeric chains and other reactants with increasing temperature, thereby leading to faster sealant degradation. In addition, temperature contributes directly to degradation by increasing the diffusion rates of oxygen and radicals, further enhancing the accessibility of oxygen and radicals for the degradation process.

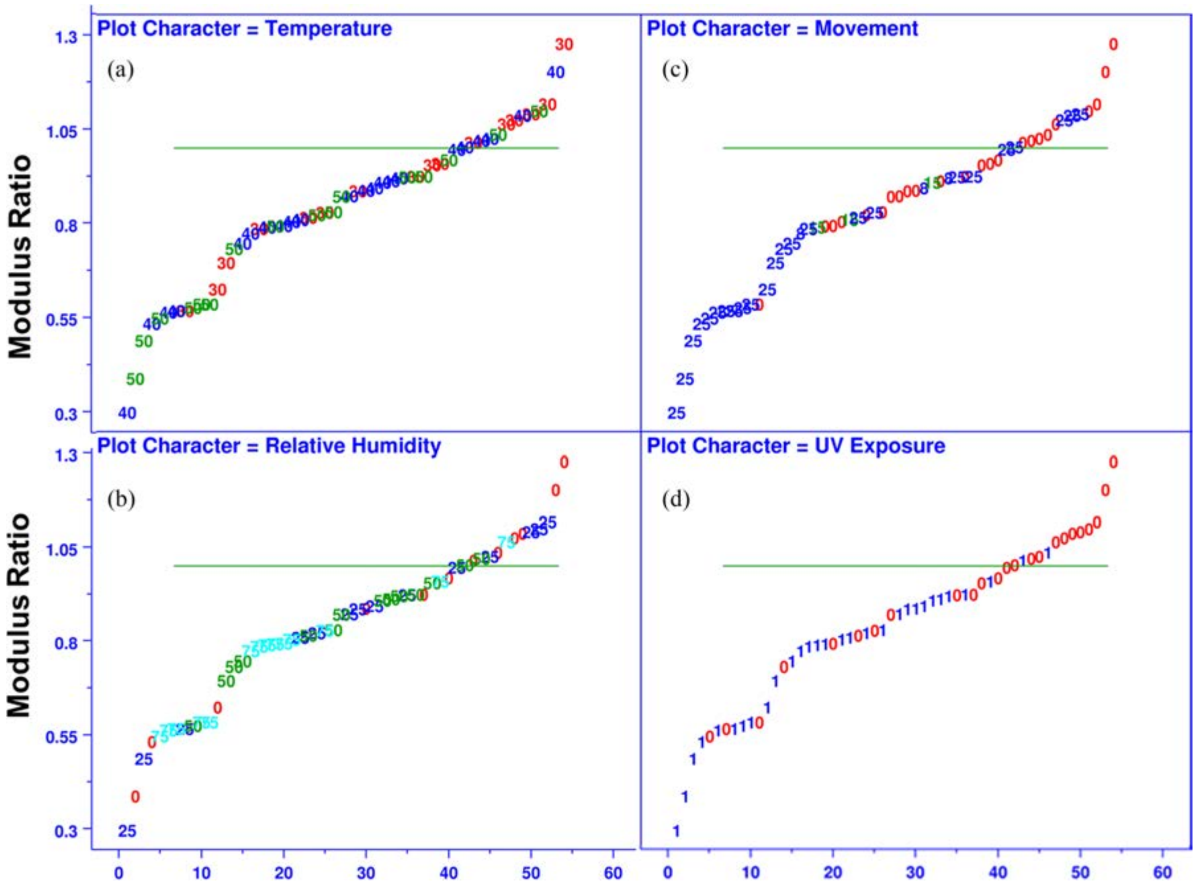

FIG. 9—*Plots of modulus ratio targeting (a) temperature, (b) RH, (c) cyclic movement, and (d) UV arranged in order of increasing magnitude for 54 distinct conditions. The deleterious effects of temperature, cyclic movement at 25 % strain, and UV can be seen from the consistent location of these variable extremes in the bottom left corner of the plots. The inconsistency of RH arrangements suggests that RH is less important.*

Effect of Moisture

The block plots of raw and averaged data targeting RH levels (i.e., 0 %, 25 %, 50 %, and 75 %) over 14 different combinations of robustness factors are shown in Figs. 10(*a*) and 10(*b*). Although the bar heights for some robustness factor settings are considerably large, the local arrangement of RH levels within each bar depends on the settings of robustness factors on the horizontal axis. Unlike temperature, RH exhibits fairly consistently large block heights but inconsistent local RH level arrangements over all settings of robustness factors. This implies that RH is a less important factor. From Fig. 10(*b*), RH levels of 50 % and 75 % resulted in the greatest modulus reduction in 7 of the 14 settings of robustness factors. Based on binomial considerations, the probability of this happening by chance is ~60 %. The usual cutoff of 5 % has not been achieved here. Therefore, this observation, coupled with the inconsistency of the effect of RH over all of the robustness factor settings, suggests that RH is statistically less important. This observation is supported further by Fig. 9(*b*), which shows that many, but not a majority, of the data points associated with 50 % and 75 % RH are located at the bottom left corner of the plot. Although the RH effect on modulus decrease is not robust or universal over various robustness factor settings, the role of RH in modulus decrease cannot be dismissed for specific exposure conditions, i.e., RH might interact with other environmental factors. The inconsistency in the local RH arrangement in each bar across all of the robustness factor settings [Figs. 10(*a*) and 10(*b*)] lends support for such a hypothesis; this is discussed in more detail shortly.

Effect of Cyclic Movement

Turning now to the effect of cyclic movement (0 %, 8 %, 15 %, and 25 % strain) on modulus change, the block plots of raw data and averaged data focusing on the movement effects of over 24 distinct robustness

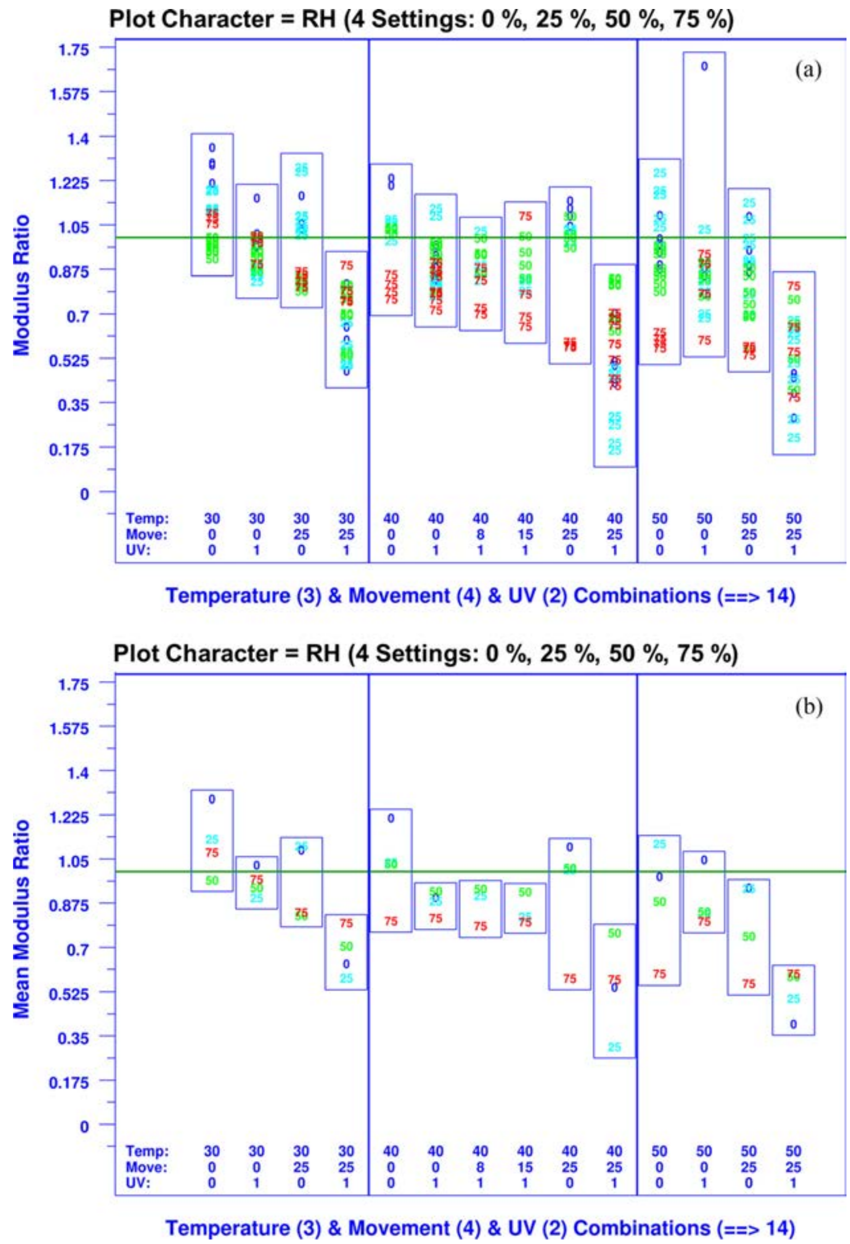

FIG. 10—*Block plot of (a) modulus ratio and (b) mean modulus ratio targeting RH across 14 distinct combinations of temperature, cyclic movement, and UV. Fairly consistently large block heights and inconsistent local RH level arrangements over all settings of robustness factors suggest that RH is a less important factor.*

factor settings are shown in Figs. 11(*a*) and 11(*b*). It is evident that all of the 20 robustness factor settings show that 25 % cyclic movement results in the greatest decrease in modulus. The probability of this happening randomly according to the binomial distribution is virtually zero ($<1 \times 10^{-4}$ %). Thus, the overall pattern of modulus decrease due to 25 % movement is unlikely to stem from random occurrence. Indeed, as shown in Fig. 9(*c*), the data for 25 % movement are always located to the bottom left of the plots. Further, the height of each block in Figs. 11(*a*) and 11(*b*) is large, signifying the prevalence of local effects of movement on modulus decrease. Such consistencies in terms of the local arrangement of 25 % movement within each bar and the large block heights over all settings of robustness factors show the deleterious effect of cyclic movement on modulus reduction. Interestingly, cyclic movements at 8 % strain and 15 % strain do not seem to affect the modulus. In fact, the modulus ratios at these values are similar to those in the tests without cyclic movement. This observation suggests that there might be a threshold value of cyclic strain below which the modulus is not affected.

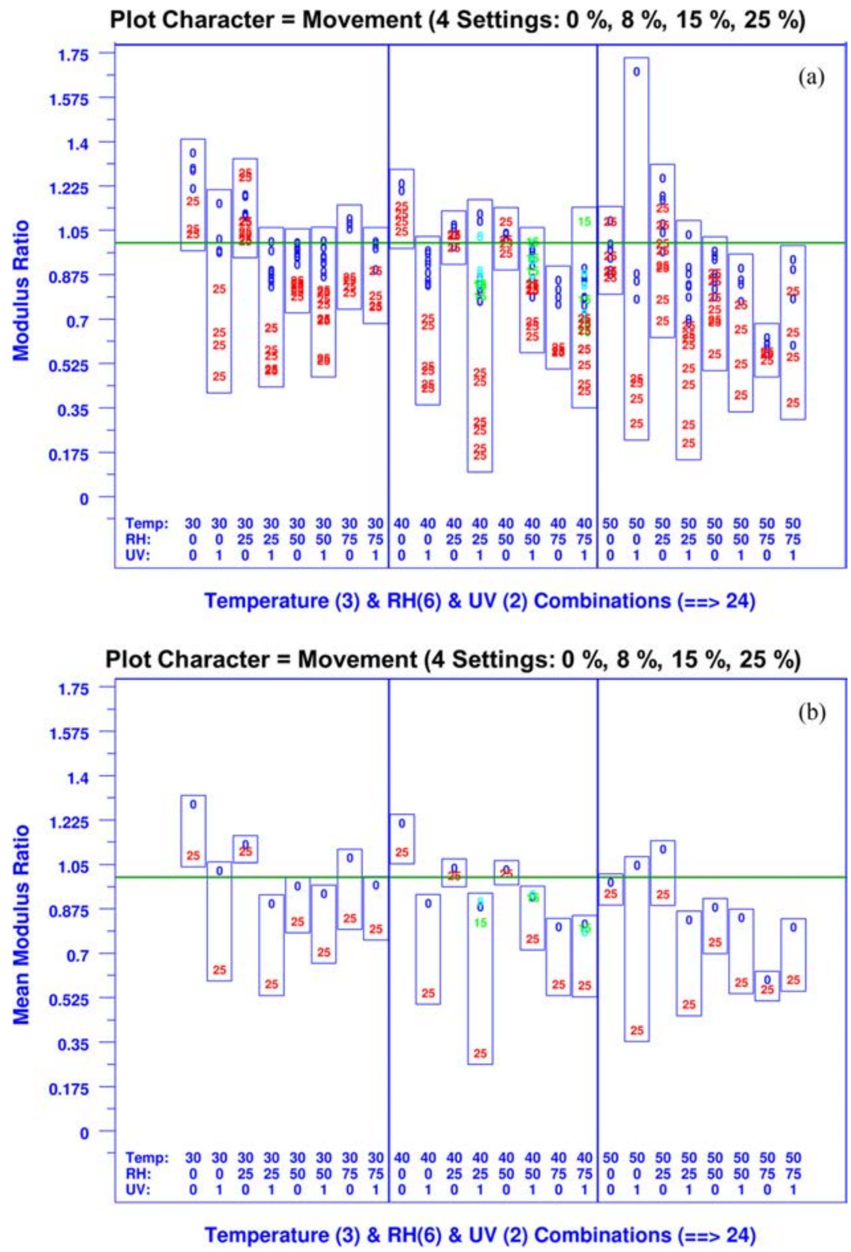

FIG. 11—*Block plot of (a) modulus ratio and (b) mean modulus ratio targeting cyclic movement across 24 distinct combinations of RH, cyclic movement, and UV.*

To date, the incorporation of cyclic movement during exposure has not been widely used in routine outdoor testing of sealants, despite the fact that a number of studies [31–35] have shown that accelerated aging under cyclic movement simulates the effects of in-service environments more closely. For the sealants studied here, the incorporation of cyclic movement in the durability tests not only will enable the use of an appropriate combination of environmental factors that closely simulates in-service conditions, but also yields an even greater acceleration factor to reduce test times for commercial sealants with a usual target service life of 20 years. It should be noted, however, that in some types of sealants the effect of cyclic movement does not greatly accelerate degradation, or it even has a negligible effect. For example, in a study by Enomoto et al. [36], mechanical cycling during outdoor exposure had no effect on the rate of degradation of two-part polyurethane and two-part silicone modified polyether (general purpose) sealants, and only a small effect on one-part polyurethane sealants.

Effect of UV

A block plot of the modulus ratio targeting UV is shown in Fig. 12(*a*). An examination of the arrangement of UV ("1") and no UV ("0") within each block shows that UV radiation is always located at the bottom

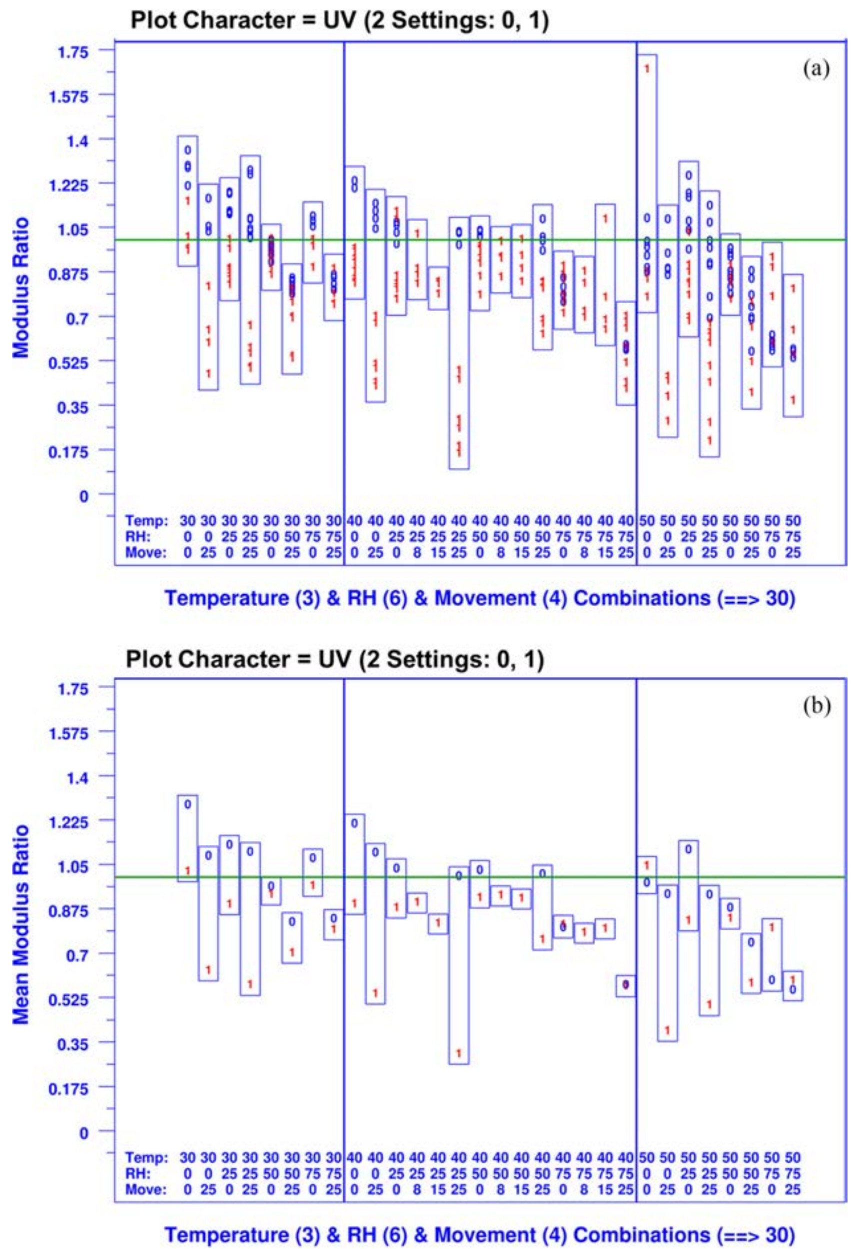

FIG. 12—*Block plot of (a) modulus ratio and (b) mean modulus ratio targeting UV across 30 distinct combinations of RH, cyclic movement, and temperature. The UV settings of "0" and "1" denote with and without UV exposure, respectively. The importance of UV in modulus decrease is evident from the consistently large block height and local arrangement of UV across the various combinations of robustness factors.*

of each bar, with the modulus ratios below unity. The block plot of the mean modulus ratio [Fig. 12(*b*)] indicates that 27 of 30 different robustness factor settings show that UV is an important factor in the modulus reduction. Based on binomial considerations, the probability of getting at least 27 of the 30 total settings by chance is 4×10^{-4} %, showing that the role of UV in modulus decrease is statistically significant. In addition, the importance of UV in modulus reduction is further attested to by the consistently large block heights across the various combinations of robustness factors [Figs. 9(*d*), 12(*a*), and 12(*b*)] in that most modulus data for UV exposure are below unity and located at the bottom left corner of the plot. Thus, it is concluded that UV is statistically important across the various robustness factor settings.

The effect of UV in decreasing modulus may be understood based on the fact that UV photons have sufficient energy to rupture the polymeric bonds present in the sealant. Because the sealant chemistry is unknown, it is impossible to propose the exact mode of chain scission. However, it is believed that UV photons are absorbed by chromophores, which are introduced into the polymer backbone during manufacturing in aliphatic type and aromatic type polymers. The chemical structures of the latter contain chromophores capable of absorbing the UV photons, which split the covalent bonds to produce free radicals. The excited chromophores then dissipate the photon energy via chain scission, leading to the rupturing of molecular bonds. The low molecular weight fragments produced by scission reactions directly correlate with the decrease in modulus.

The Worst Factor for Modulus Decrease

We have identified temperature, cyclic movement, and UV radiation as statistically significant factors for modulus decrease over all robustness factor settings, but determining which factor is the most important among these three is also of interest. This determination is done by deciding which plot has the consistently largest block heights, along with consistent arrangement within blocks showing the target factor located at the bottom of each bar. An examination of all block plots leads to the identification of cyclic movement as the most important factor for modulus decrease, followed by UV and temperature; RH is the least important factor. This ranking is consistent with that obtained from the dex plots. In a study of various latex and solvent-borne acrylic sealant products, Karparti [37] also discovered that cyclic movement was the major aging factor during outdoor exposure, and that outdoor weathering without cyclic movement alone had a negligible effect. This systematic laboratory approach clearly reveals the importance of cyclic movement in the degradation of sealants in a quantitative manner.

Although the results here suggest that cyclic movement is the most important factor in degrading the sealants, followed by UV, this should not be misinterpreted as meaning that cyclic movement causes the degradation of sealants in the absence of UV. This is not true for the sealant in this study, based on the information in the next section, and it would not be true for most sealants currently in use. For most polymeric materials, UV is required in order to initiate degradation because it has sufficient energy to break many types of polymeric chemical bonds, which leads to secondary reactions promoted by other environmental factors. For applications of building sealants in which movement has a significant effect on deterioration, the addition of cyclic movement to the exposure test is essential in order to promote the type of failure produced during in-service application of the sealant as a secondary reaction following initiation by radiation.

Interaction of Environmental Variables

Thus far, the effect of individual target factors on the decrease of the modulus has been examined over various robustness factor combinations. In investigating the interaction of robustness factors, a comparison among external block-to-block differences is performed. From the plot of average modulus ratios targeting RH [Fig. 10(*b*)], the effect of RH in decreasing the modulus ratio is seen for exposures without UV, and vice versa. For instance, high RH levels always reside at the bottom of each bar for 50°C/25 % movement/UV, whereas low RH levels are located at the bottom of each bar for 50°C/25 % movement/no UV. Furthermore, a close examination of the results for 50°C over all levels of cyclic movement and RH reveals that with UV exposure, the modulus decrease depends on the level of cyclic movement, but the humidity effect is small. Without UV, humidity has a greater effect than cyclic movement. Indeed, high RH levels are found at the bottom of each bar in all six settings involving combinations of temperature and movement without UV. Ignoring the bars showing a small local RH level effect, low RH levels with the presence of UV are located at the bottom of each bar in five of six different settings involving different temperatures and movement with UV. These results suggest that the interaction between UV and RH is significant in that UV seems to overwhelm the effect of moisture.

The negligible effect of humidity on modulus decrease for specimens exposed to UV prompts an examination of the interactions between temperature and motion. The block plots in Figs. 8 and 11 reinforce the two conclusions drawn from Fig. 6. First, the individual effect of temperature or cyclic movement is significant, as shown by the progressive decrease in modulus with increasing magnitudes of cyclic movement or temperature. Second, the combination of temperature and cyclic movement produces even greater effects. In particular, a modulus decrease of >75 % is observed for 50°C/25 % movement. This also can be seen in Table 2, which is simply a rearrangement of the data that groups temperature and cyclic movement on the vertical axis and RH level and UV on the horizontal axis. The combinations of elevated temperatures and 25 % movement always are located at the top left corner of the table, showing

TABLE 2—Data rearrangement grouping temperature and cyclic movement on the vertical axis and RH level and UV on the horizontal axis.

Temperature (3) and Movement (4)	Relative Humidity (4) and UV (2)								
	25,1	75,0	0,1	75,1	50,1	50,0	25,0	0,0	Mean
50,25	0.49	0.55	0.39	0.59	0.58	0.74	0.93	0.93	0.65
40,25	0.30	0.57	0.54	0.57	0.75	1.01	1.00	1.09	0.73
30,25	0.57	0.83	0.63	0.79	0.70	0.82	1.10	1.08	0.82
40,15	0.82			0.79	0.91				0.84
40,8	0.90			0.78	0.93				0.87
50,0	0.83	0.59	1.04	0.80	0.84	0.88	1.10	0.97	0.88
40,0	0.88	0.80	0.89	0.81	0.92	1.02	1.03	1.21	0.94
30,0	0.89	1.07	1.02	0.96	0.93	0.96	1.12	1.28	1.03
Mean	0.71	0.74	0.75	0.76	0.82	0.90	1.05	1.09	0.84

the deleterious effect of combining UV radiation, cyclic movement, and elevated temperature. Indeed, this combination of environmental variables is the worst setting for modulus decrease. This is consistent with a prior study on two sealants with different formulations, which showed that sealant joints were able to resist the individual influence of cyclic movement, high temperature, or RH but degraded substantially when exposed to a combination of cyclic movement and high temperature or RH, or a combination of these three factors [1].

The simultaneous application of UV and cyclic movement has a pronounced effect on crack formation in sealants. As shown in Fig. 13, small, deep cracks are visible on the surface of specimens exposed to 50°C/75 % RH/UV/25 % cyclic movement, but fewer shallow cracks ae observed in the specimens under the same conditions but without cyclic movement. These observations imply that exposure without cyclic movement results in only surface degradation, and that simultaneous cyclic movement during weathering accelerates the bulk deterioration of sealants. Notably, specimens under similar conditions without UV did not exhibit any cracking. This indicates the significant deleterious impact of UV exposure and cyclic movement on the aging of this particular sealant. Cyclic tensile stress might promote the penetration of UV into the sealants and enable microcrack initiation in the degraded polymer surface layer to propagate into the bulk sealants. In contrast, cyclic compressive loads might lead to the alignment of molecular segments and the packing of molecules such that the ease of UV penetration into the sealant is reduced and sealant degradation is minimized. This is a subject for further study.

It is recognized that the relative effects of the various environmental factors on the properties of the sealant can differ with the type of base polymer in the sealant, other components included in the formulation, and impurities and reaction products. Each ingredient reacts to the various environmental factors in different ways, so the relative effects of stresses will vary from one sealant formulation to another. The present study presents findings based on tests with a single sealant; however, the experimental protocol could be applicable to broad classes of materials.

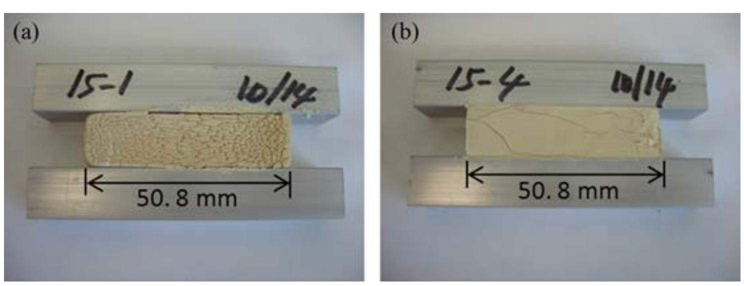

FIG. 13—*Appearance of representative test specimens exposed to the combination of 50°C, 75 % RH, and UV radiation (a) with 25 % cyclic movement and (b) without cyclic movement. Exposure without cyclic movement results in only surface degradation, whereas simultaneous cyclic movement during weathering accelerates the bulk deterioration of sealants.*

Conclusions

The accurate prediction of in-service performance in less time than is required for field tests and tests on structures has been hindered by a poor understanding of the failure modes in the two environments, a lack of methods for accurately quantifying the effects of environmental degradation factors, and crude techniques for monitoring sealant degradation. In this study, a reliability-based approach was implemented in order to systematically assess the individual and synergistic impacts of four major environmental factors (temperature, cyclic movement, UV exposure, and RH) on a sealant system. This methodology utilized laboratory exposure devices that allowed accurate control and monitoring of these environmental factors, as well as a quantitative measurement procedure for characterizing sealant degradation. Changes in the modulus were used as an indicator of the effects of environmental factors because a decrease in the modulus was found to be a precursor to cracking and debonding in our sealant system, which allow moisture penetration (the usual definition of failure). Because each material responds differently to environmental factors, the modulus should not be viewed as a universal performance indicator for all sealants. The main conclusions are summarized as follows:

1. Elevated temperature is statistically significant for decreasing modulus irrespective of the robustness factor settings (i.e., cyclic movement, RH, and UV radiation).
2. Cyclic movement at 25 % strain is statistically significant for decreasing modulus irrespective of the robustness factor settings (i.e., temperature, RH, and UV radiation). However, unlike with 25 % strain, cyclic movement at 8 % and 15 % strain does not have any impact on the modulus. This observation suggests that there might be a threshold value of cyclic strain below which the effect of strain is negligible.
3. UV is statistically significant for decreasing modulus irrespective of the robustness factor settings (i.e., cyclic movement, RH, and temperature).
4. RH seems less important for decreasing modulus irrespective of the robustness factor settings (i.e., cyclic movement, temperature, and UV radiation).
5. UV radiation suppresses the effect of RH on modulus decrease. In the absence of UV, RH has a greater effect than cyclic movement.
6. Among various environmental factors, cyclic movement at 25 % strain is the most important factor for modulus decrease, followed by UV radiation, temperature, and RH.
7. The combination of cyclic movement and temperature produces a synergistic effect leading to a larger reduction in modulus than that seen with either variable alone.

Acknowledgments

The support from a NIST/industry consortium on Service Life Prediction of Sealant Materials is greatly appreciated. Participating companies include DAP, Degussa, Dow Corning, Kaneka Texas, SIKA, Solvay, Tremco, and Wacker Silicones.

References

[1] Woolman, R. and Hutchinson, A., *Resealing of Buildings: A Guide to Good Practice*, Butterworth-Heinemann, Oxford, UK, 1994.

[2] Grunau, E., "Service Life of Sealants in Building Construction" (in German), Research Report, Federal Ministry for Regional Planning, Building and Urban Planning, Bonn, Germany, 1976.

[3] Chiba, R., Wakimoto, H., Kadono, F., Koji, H., Karimori, M., Hirano, E., Amaya, T., Sasatani, D., and Hosokawa, K., *Improvement System of Waterproofing by Sealants in Japan*, Japan Sealant Industry Association, Tokyo, Japan, 1992, pp. 175–199.

[4] *Durability of Building and Construction Sealants and Adhesives*, STP 1453, A. T. Wolf, Ed., ASTM International, West Conshohocken, PA, 2004, pp. 385–398.

[5] Martin, J. W., Nguyen, T., and Wood, K. A., *Service Life Prediction—Challenging the Status Quo*, J. W. Martin, R. A. Ryntz, and R. A. Dickie, Eds., Federation of Societies for Coatings Technology, Blue Bell, PA, 2005, p. 13.

[6] Fischer, R. M., Ketola, W. D., and Murray, W. P., *Prog. Org. Coat.*, Vol. 19, 1991, p. 165.

[7] ASTM C1519-10, "Standard Test Method for Evaluating Durability of Building Construction Sealants by Laboratory Weathering Procedures," *Annual Book of ASTM Standards*, ASTM International, West Conshohocken, PA.

[8] ISO 11431:2002, "Building Construction—Jointing Products—Determination of Adhesion/Cohesion of Sealants after Exposure to Heat, Water and Artificial Light through Glass."

[9] ISO 11600:2002, "Building Construction—Jointing Products—Classification and Requirements for Sealants."

[10] White, C. C., Tan, K. T., Hunston, D. L., and Williams, R. S., *Service Life Prediction of Polymeric Materials: Global Perspective*, J. W. Martin, R. A. Ryntz, J. Chin, and R. Dickie, Eds., Springer, New York, 2008, pp. 115–128.

[11] Tan, K. T., White, C. C., Benatti, D. J., and Hunston, D. L., *Service Life Prediction for Sealants Industry/Government Consortium Technical Report: Precision Exposure Chambers and Screening Experiments*, C. C. White, Ed., 2007, pp. 127–155.

[12] Tan, K. T., White, C. C., Benatti, D. J., Stanley, D., and Hunston, D. L., *Handbook of Sealant Technology*, K. L. Mittal and A. Pizzi, Eds., CRC Press, Boca Raton, FL, 2009, pp. 75–92.

[13] White, C. C., Hunston, D. L., and Tan, K. T., *J. ASTM Int.*, Vol. **6**(2), 2009.

[14] Lacher, S., Williams, R. S., Halpin, C., and White, C. C., *Service Life Prediction—Challenging the Status Quo*, J. W. Martin, R. A. Ryntz, and R. A. Dickie, Eds., Federation of Societies for Coatings Technology, Blue Bell, PA, 2005, pp. 207–216.

[15] Williams, R. S., Lacher, S., Halpin, C., and White, C. C., *Service Life Prediction—Challenging the Status Quo*, J. W. Martin, R. A. Ryntz, and R. A. Dickie, Eds., Federation of Societies for Coatings Technology, Blue Bell, PA, 2005, pp. 171–185.

[16] Tan, K. T., White, C. C., Benatti, D. J., and Hunston, D. L., *Polym. Degrad. Stab.*, Vol. **93**, 2008, pp. 648–656.

[17] Tan, K. T., White, C. C., Benatti, D. J., and Hunston, D. L., *Polym. Degrad. Stab.*, Vol. **95**, 2010, pp. 1551–1556.

[18] White, C. C., Tan, K. T., Hunston, D. L., Benatti, D. J., Nguyen, T., Stanley, D., and Chin, J. W., *Polym. Degrad. Stab.*, Vol. **96**, 2011, pp. 1104–1110.

[19] White, C. C., Tan, K. T., O'Brien, E. P., Hunston, D. L., Chin, J. W., and Williams, R. S., *Rev. Sci. Instrum.*, Vol. **82**, 2011, 025112.

[20] White, C. C., Hunston, D. L., Tan, K. T., Hettenhouser, J., and Garver, D. J., "An Accelerated Exposure and Testing Apparatus for Building Joint Sealants," *Rev. Sci. Instrum.* (submitted)

[21] Wolf, A. T., *Proceedings of the Sealant Technology Conference*, Oxford Brookes University, School of Technology, Oct. 13, 2004.

[22] ASTM C719.

[23] Chin, J. W., Byrd, E., Embree, N., Garver, J., Dickens, B., Finn, T., and Martin, J., *Rev. Sci. Instrum.*, Vol. **75**, 2004, p. 4951.

[24] ASTM G173-03.

[25] Taylor, C. R., Greco, R., Kramer, O., and Ferry, J. D., *J. Rheol.*, Vol. **20**, 1976, pp. 141–152.

[26] Ferry, J. D., *Viscoelastic Properties of Polymers*, 3rd ed., John Wiley & Sons, Inc., New York, 1980.

[27] Ketcham, S. A., Niemiec, J. M., and McKenna, G. B., *J. Eng. Mech.*, Vol. **122**, 1996, pp. 669–677.

[28] National Institute of Standards and Technology, 2003, *NIST/SEMATECH e-Handbook of Statistical Methods*, NIST Handbook 151, http://www.itl.nist.gov/div898/handbook/

[29] Filliben, J. J., *Proceedings of the Indo-U.S.-Japan Conference: Quality through Engineering Design*, W. Kuo, Ed., Elsevier, Amsterdam, 1993, pp. 199–223.

[30] Filliben, J. J., "Dataplot—Introduction and Overview," *NBS Special Publication 667*, National Bureau of Standards, Washington, D.C., 1984.

[31] Searle, N. D., *Handbook of Sealant Technology*, K. L. Mittal and A. Pizzi, Eds., CRC Press, Boca Raton, FL, 2009, pp. 93–142.

[32] Wolf, A. T., *Handbook of Sealant Technology*, K. L. Mittal and A. Pizzi, Eds., CRC Press, Boca Raton, FL, 2009, pp. 143–189.

[33] Beech, J. C., *Mater. Struct.*, Vol. **18**, 1985, pp. 473–482.

[34] Jones, T. G. B. and Lacasse, M. A., "Durability of Building Sealants," *RILEM Report 21*, A. T. Wolf, Ed., RILEM Publications, Paris, 1999, pp. 73–105.

[35] Wolf, A. T., "Durability of Building Sealants," *RILEM Report 21*, A. T. Wolf, Ed., RILEM Publications, Paris, 1999, pp. 365–380.

[36] Enomoto, N., Ito, A., Shimizu, I., Matsumura, T., Takane, Y., and Tanaka, K., *J. ASTM Int.*, Vol. **4**, (2), 2007.

[37] Karpati, K. K., *Adhesive Age*, Vol. **23**(1), 1980, pp. 41–47.